Hybridization Probes

DOI: 10.1002/anie.201005902

Fluorescence Imaging of Influenza H1N1 mRNA in Living Infected Cells Using Single-Chromophore FIT-PNA**

Susann Kummer, Andrea Knoll, Elke Socher, Lucas Bethge, Andreas Herrmann, and Oliver Seitz**

In light of the increasing importance assigned to RNA, significant efforts have been devoted to the development of fluorescent oligonucleotide probes that allow the imaging of RNA expression in living cells.[1] Molecular beacons[2] (MBs, Scheme 1 a) probably are amongst the most widely used probes for RNA imaging.[3] These hairpin-shaped probes rely on the interaction between two terminally appended chromophores which are separated upon formation of probe–target complexes. Unintended protein binding and/or nuclease-mediated probe degradation can also affect the distance between the chromophores.[4]

We have introduced so-called FIT-PNA probes[5] (Scheme 1 b), which contain a single thiazole orange (TO) intercalator serving as artificial fluorescent nucleobase. These probes respond to changes of the local structure in the vicinity of the dye rather than to the more global changes of conformation that confer fluorescence signaling by the dual-labeled molecular beacons.[6] High fluorescence enhancements require intercalation of the TO dye. This is expected to help in avoiding strong fluorescence signals upon inevitable binding to proteins. Amongst the many TO-containing probes reported[7] FIT probes are unique because a single fluorophore provides for both high enhancements of fluorescence upon matched hybridization and high target specificity at nonstringent hybridization conditions where both matched and mismatched probe–target complexes coexist. Further assets are the high affinity of the PNA probes for complementary RNA and the enhanced biostability provided by the peptide nucleic acid (PNA) backbone.[8] Herein we demonstrate the advantageous properties of FIT-PNA probes in the imaging of mRNA from an influenza virus strain belonging to the same subtype as the recently emerged swine virus (A/Mexico/1/2009, H1N1).

In a research program aiming at the characterization of the spatio-temporal pattern of virus assembly, we required a method that enables imaging of the mRNA coding for neuraminidase of influenza virus A/PR/8. FIT probes such as **1a** and **1b** were designed to target a sequence in the NA mRNA (nt 599–615, referred to the accession number NC_002018) which is essentially sequence identical to the NA mRNA from A/Mexico/1/2009/swine (H1N1, nt 625–640) (Figure 1). The accessibility of the target segment, which can be hindered by RNA folding and binding of proteins, has been previously demonstrated by Zhang and co-workers.[9] A rapid screen, which required the synthesis[10] of eight different PNA oligomers, suggested FIT probe **1a** as a suitable probe (see the Supporting Information). This sensor provided an 11-fold increase of the TO emission upon hybridization with complementary RNA target **3a** at 37 °C (Figure 2 a). Furthermore, we tested the subtype specificity. The RNA **4** from a different influenza strain (NA mRNA from A/X-31, H3N2, nt 16–32) includes seven continuous matched base pairs around the thiazole orange "base". Nevertheless, the fluorescence of **1a** remained virtually unchanged when RNA **4** was added. The TMR/Dabcyl-labeled molecular beacon **2** (Figure 1; TAMRA = tetramethyl-6-carboxyrhodamine; Dabcyl = 4-(4-dimethylaminophenyl)diazenylbenzoic acid) was used in a

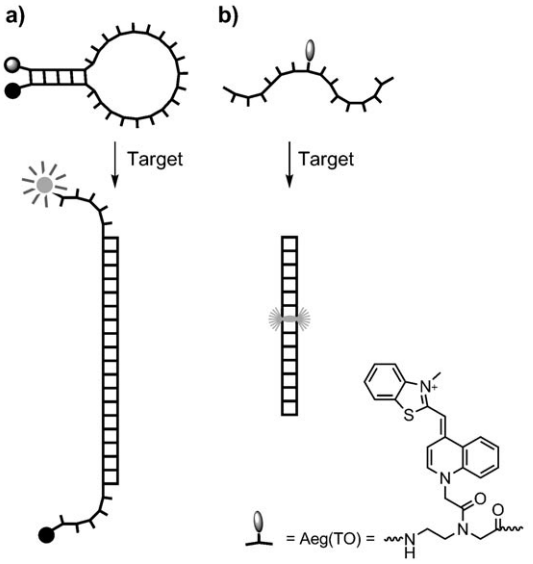

Scheme 1. Nucleic acid detection with a) molecular beacon probes (MBs) and b) FIT-PNA probes. MBs change conformation upon binding of a complementary target. In FIT-PNA probes, an intercalator dye such as thiazole orange (TO) responds to changes of the local environment. Stacking interactions hinder twisting around the TO methine bridge and thus confer enhancements of fluorescence.

[*] Dr. A. Knoll, Dr. E. Socher, L. Bethge, Prof. Dr. O. Seitz
Department of Chemistry, Humboldt University Berlin
Brook-Taylor-Strasse 2, 12489 Berlin (Germany)
Fax: (+49) 30-2093-7266
E-mail: oliver.seitz@chemie.hu-berlin.de
S. Kummer, Prof. Dr. A. Herrmann
Department of Biology, Humboldt University Berlin
Invalidenstrasse 42, 10115 Berlin (Germany)
Fax: (+49) 30-2093-8585
E-mail: andreas.herrmann@rz.hu-berlin.de

[**] This work was financially supported by grants from the Deutsche Forschungsgemeinschaft (to A.H. and O.S.).

Supporting information for this article is available on the WWW under http://dx.doi.org/10.1002/anie.201005902.

FIT-PNA probes
1a, H-Lys-cagtta-Aeg(TO)-tatgccgttg-Lys-NH_2
1b, H-Lys(PEG)-cagtta-Aeg(TO)-tatgccgttg-NH_2
1c, H-Lys(PEG)-cgttt-Aeg(TO)-taattcgtctc-Lys-NH_2

Molecular Beacon
2, TMR-GCGACTTTCAGTTATTATGCCGTTGTATTTGTCGC-Dabcyl

RNA targets
3a, 5'-CAACGGCAUAAUAACUG-3', A/PR/8 (H1N1), nt 599-615
3b, 5'-AAAUACAACGGCAUAAUAACUGAAA-3', A/PR/8 (H1N1, nt 594-618)
3c, 5'-UCAAAAGAUAAUAACAA-3', A/X-31 (H3N2, DQ87 4878, nt 16-32)

Lys(PEG) = 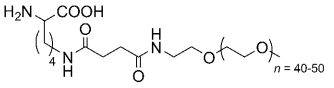

Figure 1. Probe molecules and targets used in this study. Nucleotides are indicated referring to the accession number NC_002018 (A/PR/8, H1N1) if not stated otherwise.

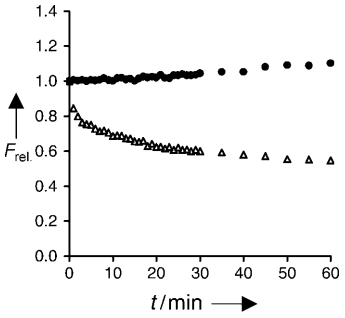

Figure 3. Relative fluorescence ($F(t)\,F_0(t{=}0)/F(t{=}0)\,F_0(t)$) from FIT-PNA **1a** (●) and MB **2** (△) in cell lysates upon addition of target RNA **3a** and **3b**, respectively. $F(t)$, $F_0(t)$ = fluorescence in presence or absence of target RNA, respectively, measured at λ_{ex} = 485 nm, λ_{em} = 530 nm for FIT-PNA or λ_{ex} = 559 nm, λ_{em} = 593 nm for MB. Conditions: 1 μM probe, 10 μM RNA in 100 μL cell lysate, 37 °C.

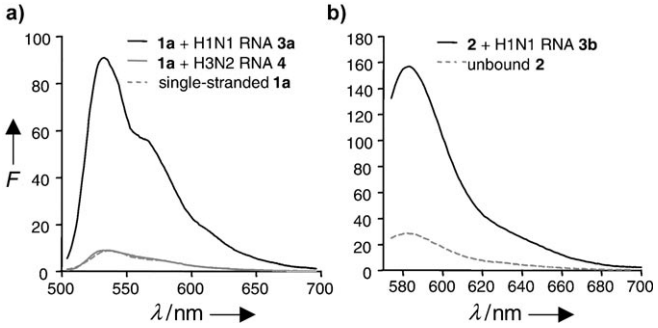

Figure 2. Fluorescence spectra of a) FIT-PNA **1a** (λ_{ex} = 485 nm) and b) MB **2** (λ_{ex} = 559 nm) before and after addition of matched H1N1 RNA or mismatched H3N2 RNA at 37 °C. Conditions: 1 μM probe and 10 μM target in 100 mM NaCl, 10 mM NaH_2PO_4, pH 7.0.

previous imaging study.[9] This probe provided sixfold enhancement of TAMRA emission upon addition of the complementary RNA **3b** (Figure 2b).

We next compared FIT probe **1a** and DNA molecular beacon **2** in the detection of RNA in cell lysates. The lysates from MDCK cells were spiked with the complementary RNA target **3b** or with buffer and the probes were added. The responsiveness F/F_0 (F, F_0 = fluorescence intensity of RNA-containing or control lysates, respectively) of the molecular beacon decreased by more than 40% after only 60 min exposure to the cell lysate (Figure 3). This result can be caused by nuclease-mediated degradation and protein binding, which both would lead to increases of F_0 in the absence of target (Figure S24). By contrast, the increase of fluorescence F/F_0 provided by FIT probe **1a** remained high, regardless of the duration of exposure. We concluded that FIT probe **1a** is stable in lysates and probably also in living cells. A further control experiment was performed in order to assess whether FIT probes recognize double-stranded DNA. We incubated probe **1a** with calf-thymus duplex DNA at a 100-fold excess of base pairs, a situation that is unlikely to occur in live-cell studies of cytosolic RNA (Figure S25). Even under these conditions, the FIT probe **1a** remained responsive and still showed strong increases of fluorescence upon addition of the RNA target at a slightly increased background. Unselective intercalation of the "tether-free" TO–PNA linkage into DNA base pairs is probably hindered for steric reasons.

In preparation for the live-cell imaging studies, we used quantitative real-time polymerase chain reaction (qPCR) to assess the progression of the viral mRNA production during the infection cycle of A/PR/8 in MDCK cells. After infection[9] the total RNA was extracted, reversibly transcribed, and studied by qPCR (Figure S26). FIT-PNA **1a** enabled quantification because the target-induced fluorescence increase was high at both 37 °C and 60 °C, an option that is not offered by "conventional" molecular beacons (Figure S23). The results of the qPCR analysis exposed that the virus required 4–5 h postinfection to attain maximal levels of approximately 10^4 copies of NA mRNA per infected cell.

The next goal was to detect the viral mRNA in living cells. An oligoethyleneglycol chain was attached to FIT probe **1b** to prevent segregation and nuclear import.[11] A succinylaminoethyl-*O*-methylpolyethylene glycol group was coupled with lysine-modified PNA in solution by using the *N*-hydroxysuccinimide active ester (see the Supporting Information). The PEGylation had negligible effects on the fluorescence properties (compare Figures S13, S20, and S21). Probe **1b** was introduced into living MDCK cells utilizing streptolysine O (SLO)-mediated permeabilization of the plasma membrane as previously described.[9] The intact morphology of the cells and the lack of staining by propidium iodide attested to the vitality of the SLO-treated cells (Figure S30). A 250 nM concentration of **1b** was sufficient to achieve delivery and specific labeling. Prior to imaging, the cells were resealed for additional 30 min. A 488 nm argon laser was used for excitation of the TO chromophore and the emission was measured in a range of 510–540 nm. In the confocal laser scanning microscopy (CLSM) images of cells that were infected by influenza A/PR/8 intensive fluorescence was observed (Figure 4a). By contrast, noninfected control cells showed weak/insignificant fluorescence (Figure 4b). For quantitative analysis, regions of interest were manually selected (Figure S28). The intracellular fluorescence intensity of different cells was determined and the background intensity subtracted. The image analysis revealed that influenza H1N1 infected cells fluoresced with 4.5-fold higher

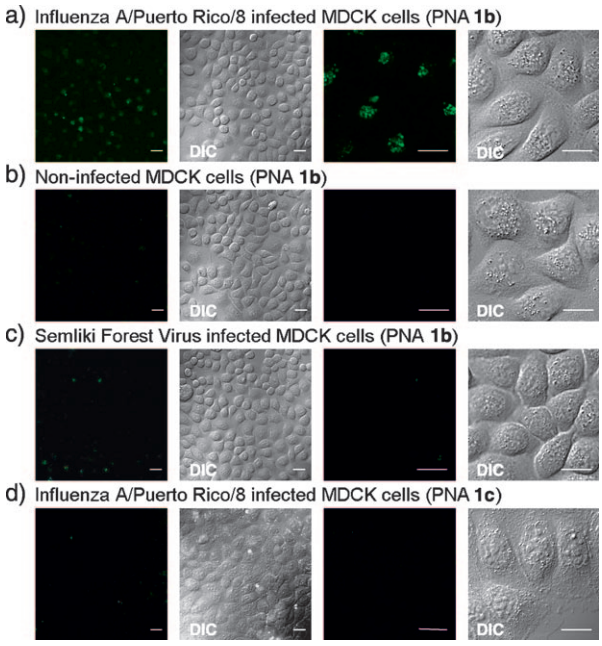

Figure 4. a–d) Confocal laser scanning microscopy images of living MDCK cells stained with the FIT-PNA probe **1b** specific for influenza A/Puerto Rico/8 NA (a–c) or the FIT PNA probe **1c** specific for vesicular stomatitis virus L (d) 4.5 h after infection (M.O.I. = multiplicity of infection 100). FIT-PNAs were excited with a 488 nm argon ion laser in living MDCK cells. Images were recorded with an inverted confocal laser scanning microscope at 37 °C and $\lambda_{ex} = 488$ nm. The two sets of panels on the right represent a threefold magnification of the left two. White bars: 10 μm. (DIC = differential interference contrast).

intensity than the noninfected cells (Figure 5). We included two further controls to assess whether probes such as **1b** unselectively respond to the increased mRNA transcription levels that may accompany virus infection. For this purpose, cells were infected with Semliki Forest virus (SFV; Figure 4c).

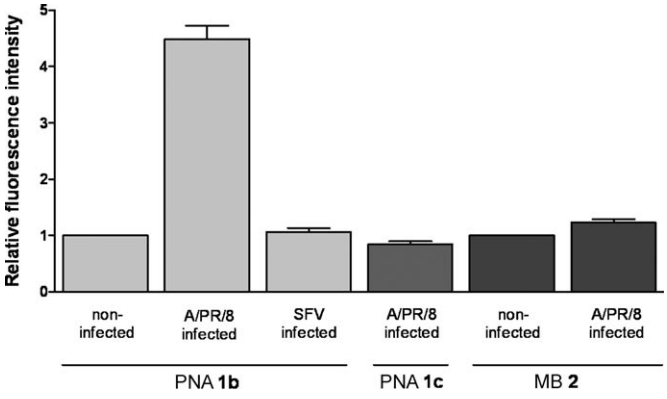

Figure 5. Relative fluorescence intensity of FIT-PNA **1b** in influenza A/Puerto Rico/8 NA infected MDCK cells, noninfected (control) MDCK cells, and Semliki Forest Virus infected MDCK cells as well as of PNA **1c** and molecular beacon **2** in influenza A/Puerto Rico/8 NA infected MDCK cells. Integrated fluorescence intensity values of all samples are normalized to the mean of the control and indicated as bars. Scatter bars correspond to the standard error of the mean. Data represent three independent experiments with five cells per experiment ($n = 15$).

The SFV-infected cells showed modest 1.1-fold increases of fluorescence (Figure 4c and Figure 5). Additionally, FIT-PNA **1c** specific to the mRNA encoding for the L protein of vesicular stomatitis virus, an RNA-dependent RNA polymerase (VSV, target sequence: nt 9109-9124 referred to the accession number NC_001560, Figure 1), was measured in influenza H1N1 infected MDCK cells. This probe **1c** fluoresces upon hybridization with VSV RNA, yet is virtually nonresponsive to the addition of the H1N1 RNA **3a** (Figure S22). The live-cell confocal microscopy revealed no difference in fluorescence intensity compared to noninfected cells. Both control experiments demonstrated that the high fluorescence intensity of FIT-PNAs in A/PR/8-infected cells is due to the virus-specific NA mRNA.

For a comparison, molecular beacon **2** was introduced into the cells.[9] The analysis of the CLSM images (Figure S27) showed that influenza-infected cells exhibited only 1.2-fold higher intracellular fluorescence than noninfected cells. This value is within reasonable agreement with the 1.8-fold (± 30 %) higher intensity of the MB **2** fluorescence measured in a previous study for cells 4.5 h after infection (compared to 1.5 h after infection).[9] While the details of the previous image analysis of both infected and noninfected cells have not been included, we note that FIT-PNA **1b** in influenza H1N1 infected cells fluoresced with 4.5-fold (± 6 %) higher intensity than in noninfected cells at significantly reduced errors.

The fluorescence microscopy images indicate a heterogeneous, non-random intracellular distribution of NA mRNA. Although further studies are warranted to clarify whether this localization reflects also that of mRNA not in complex with FIT-PNA, mRNA is supposed to localize in subcellular compartments for regulatory, developmental, and economical purposes.[12]

DNA-based molecular beacons are amongst the most frequently used hybridization probes in live-cell RNA imaging. High sequence specificity and high hybridization-induced enhancements of fluorescence have been reported.[1b,2–4,11,13] Our data provides, to the best of our knowledge, the first example of a non-nucleotidic probe that can be used for the imaging of mRNA in living cells. PNA-based FIT probes such as **1** are not subject to degradation by either nucleases or proteases. The signal-to-background ratio provided by FIT-PNA was superior to that of a molecular beacon recently used in live-cell RNA imaging. Our study suggests that FIT-PNAs are attractive tools to study the gene regulation of processes in living cells. While we were interested here in a member of the very acute influenza virus family (H1N1), the approach can be readily applied to other viruses as well. Further studies will focus on application of FIT-PNA to quantify the expression of viral mRNA on an absolute scale at the single-cell level in real time.

Received: September 20, 2010
Revised: October 22, 2010
Published online: January 21, 2011

Keywords: confocal microscopy · hybridization probes · molecular beacons · RNA · viruses

[1] a) P. J. Santangelo, *Wiley Interdiscip. Rev. Nanomed. Nanobiotechnol.* **2010**, *2*, 11 – 19; b) G. Bao, W. J. Rhee, A. Tsourkas, *Annu. Rev. Biomed. Eng.* **2009**, *11*, 25 – 47; c) S. Paillasson, M. Van De Corput, R. W. Dirks, H. J. Tanke, M. Robert-Nicoud, X. Ronot, *Exp. Cell Res.* **1997**, *231*, 226 – 233; d) A. Tsuji, *Biophys. J.* **2000**, *78*, 3260 – 3274; e) S. Sando, E. T. Kool, *J. Am. Chem. Soc.* **2002**, *124*, 9686 – 9687; f) R. M. Franzini, E. T. Kool, *J. Am. Chem. Soc.* **2009**, *131*, 16021 – 16023; g) Z. Pianowski, K. Gorska, L. Oswald, C. A. Merten, N. Winssinger, *J. Am. Chem. Soc.* **2009**, *131*, 6492 – 6497; h) K. Furukawa, *Bioconjugate Chem.* **2009**, *20*, 1026 – 1036.

[2] S. Tyagi, F. R. Kramer, *Nat. Biotechnol.* **1996**, *14*, 303 – 308.

[3] a) D. P. Bratu, B. J. Cha, M. M. Mhlanga, F. R. Kramer, S. Tyagi, *Proc. Natl. Acad. Sci. USA* **2003**, *100*, 13308 – 13313; b) Z. Q. Cui, Z. P. Zhang, X. E. Zhang, J. K. Wen, Y. F. Zhou, W. H. Xie, *Nucleic Acids Res.* **2005**, *33*, 3245 – 3252; c) P. Santangelo, N. Nitin, L. LaConte, A. Woolums, G. Bao, *J. Virol.* **2006**, *80*, 682 – 688.

[4] a) J. J. Li, X. Fang, S. M. Schuster, W. Tan, *Angew. Chem.* **2000**, *112*, 1091 – 1094; *Angew. Chem. Int. Ed.* **2000**, *39*, 1049 – 1052; b) J. J. Li, R. Geyer, W. Tan, *Nucleic Acids Res.* **2000**, *28*, e52; c) A. K. Chen, M. A. Behlke, A. Tsourkas, *Nucleic Acids Res.* **2007**, *35*, e105.

[5] a) O. Köhler, D. V. Jarikote, O. Seitz, *ChemBioChem* **2005**, *6*, 69 – 77; b) L. Bethge, D. V. Jarikote, O. Seitz, *Bioorg. Med. Chem.* **2008**, *16*, 114 – 125; c) E. Socher, D. V. Jarikote, A. Knoll, L. Roglin, J. Burmeister, O. Seitz, *Anal. Biochem.* **2008**, *375*, 318 – 330.

[6] a) D. V. Jarikote, N. Krebs, S. Tannert, B. Röder, O. Seitz, *Chem. Eur. J.* **2007**, *13*, 300 – 310; b) V. Karunakaran, J. L. Perez Lustres, L. Zhao, N. P. Ernsting, O. Seitz, *J. Am. Chem. Soc.* **2006**, *128*, 2954 – 2962.

[7] a) N. Svanvik, G. Westman, D. Wang, M. Kubista, *Anal. Biochem.* **2000**, *281*, 26 – 35; b) U. Asseline, M. Chassignol, Y. Aubert, V. Roig, *Org. Biomol. Chem.* **2006**, *4*, 1949 – 1957; c) C. Holzhauser, S. Berndl, F. Menacher, M. Breunig, A. Göpferich, H. A. Wagenknecht, *Eur. J. Org. Chem.* **2010**, 1239 – 1248; d) S. Berndl, M. Breunig, A. Göpferich, H. A. Wagenknecht, *Org. Biomol. Chem.* **2010**, *8*, 997 – 999; e) F. Menacher, M. Rubner, S. Berndl, H. A. Wagenknecht, *J. Org. Chem.* **2008**, *73*, 4263 – 4266; f) S. Ikeda, T. Kubota, M. Yuki, A. Okamoto, *Angew. Chem.* **2009**, *121*, 6602 – 6606; *Angew. Chem. Int. Ed.* **2009**, *48*, 6480 – 6484.

[8] P. E. Nielsen, M. Egholm, R. H. Berg, O. Buchardt, *Science* **1991**, *254*, 1497 – 1500.

[9] W. Wang, Z. Q. Cui, H. Han, Z. P. Zhang, H. P. Wei, Y. F. Zhou, Z. Chen, X. E. Zhang, *Nucleic Acids Res.* **2008**, *36*, 4913 – 4928.

[10] D. V. Jarikote, O. Köhler, E. Socher, O. Seitz, *Eur. J. Org. Chem.* **2005**, 3187 – 3195.

[11] A. K. Chen, M. A. Behlke, A. Tsourkas, *Nucleic Acids Res.* **2008**, *36*, e69.

[12] K. C. Martin, A. Ephrussi, *Cell* **2009**, *136*, 719 – 730.

[13] Y. Li, X. Zhou, D. Ye, *Biochem. Biophys. Res. Commun.* **2008**, *373*, 457 – 461.

